

Three loop correction in the formation of QGP droplet

M. Jena, K. K. Gupta¹ and S. Somorendro Singh*

*Department of Physics and Astrophysics,
University of Delhi, Delhi - 110007, India*

¹ *Department of Physics, Ramjas College,
University of Delhi, Delhi-110007, India*

Quark-gluon plasma (QGP) droplet formation is re-considered with the addition of three loop correction to the earlier loop factors in the mean field potential. The correction of the three loop factor increases stability in the droplet formations of QGP at different parametrization factors of the QGP fluid and it is in better agreement in comparison to the lattice results of pressure, energy density and other thermodynamic relations. This implies that the contribution of the three loop enhances in showing the characteristic features of the QGP fluid. It shows that increasing the loop increased the strength of parametrization value which we defined earlier as a number parameter of fluid dynamics. It indicates that the model with the loop correction boosts in explaining about the formation of QGP droplet in the expansion of early universe.

PACS numbers: 25.75.Ld, 12.38.Mh

Keywords: QGP; Surface tension; Thermodynamics

I. INTRODUCTION

There are number of reports about the process of phase transition that occurred during the early universe formation. These reports are available when we study the literature of early universe evolution. In the early universe, it is believed that the matter about a few microseconds is made of free quarks and gluons and subsequently cool down over time, the matter behave as confined matter of bound quarks of hadrons [1, 2]. This short period life of free quarks and gluons is known as quark-gluon plasma (QGP). During the short period of time, the universe is highly complicated and it is very difficult to predict the exact scenarios of the universe. So many theorists and experimentalists try to do something about the detection of this complicated matter. Although studying the matter is old enough to say it has not been possible to get whole information about the critical point and the matter at high baryon density. To explain the system, a number of highly energetic laboratories have been set up around the globe to find out how the early universe was created [3, 4]. Due to these experimental facilities available in the different places, the attraction of more expertise peoples are increasing day by day to search about the matter and really become an exciting field in the present day of heavy ion collider physics [5–7]. So heavy-ion-collision is providing the update information about the QGP formation from time to time and on the basis of its reports, many scientists around the world theoretically as well as experimentally are formalising different modelings to prove the existence and characterization of the deconfined phase of QGP. Among these modelings we also attempt to develop a simple model to represent the

structure of QCD and phase transition phenomena. The model is based on the loop correction factor by creating a mean field potential among the participating particles in the system. The loop correction has already shown some details about the thermodynamical pictures of QGP and now we extend our earlier work [8] by adding the three loop factor and looking for the improvement produced by this three loop. The model creates the free energies through the different quark and gluon flow parameters forming various sizes of stable droplets. The formation of these stable droplet differs with the change of temperature and parametrization values. It indicates that droplet formation is dependent on both the parametrization value of quark and gluon and the temperature. In addition to it, the critical radius of the droplet helps in determining the surface tension as it carries an important property of liquid drop model in determining the stability of droplet formation in the system.

In this paper, we focus on the QGP droplet formation and its thermodynamical properties through the incorporation of three loop correction in mean field potential. This is however an extensive work of our earlier programs of loop corrections [8, 9]. Due to the addition of three loop term to potential the results produced are successfully able to explain the relevant properties of QGP droplets.

The paper is arranged as follows: In section *II*, we briefly construct the Hamiltonian of the system incorporating three loop correction connecting from the two loop correction factor in the potential and find the density of states of the free energies. In section *III* the free energy, thermodynamic relations and surface tension of the system symbolising the stable droplet formation of QGP are explained. In section *IV*, the analytical and numerical solutions as results are discussed. At last, a brief conclusion with the details of QGP formation are presented.

*email:sssingh@physics.du.ac.in

II. HAMILTONIAN AND DENSITY OF STATES THROUGH LOOP CORRECTIONS

The interacting potential created among quark-quark, quark-antiquark, quarks and gluons is used as mean field potential, which in turn, help us to find the density of states of the free energy. The mean field potential in perturbed QCD is normally used among the massive quarks. The same technique of finding the mean field potential is applied among the mass-less quarks as the mass is considered as quasi-model of temperature dependent quark mass. It is because of the fact that the system is involving at very high temperature and its effect is not negligible at all in the system. There is hence contribution of interacting potential in the mean field potential due to the temperature dependent quark mass. Therefore from one loop to three loop correction among the internal quarks are required for the calculation of the actual interacting potential. The contributions of these terms are also already reported earlier by our works. So we use the effective mean field potential produced by all these loop correction factors in determining the density of states similar to our earlier papers [10, 11]. Due to three loop correction we get an improved results in all the thermodynamic parameters. Now Hamiltonian of the confining/de-confining potentials among the particles is formulated with the addition of three loop to the earlier loops and hence it leads in obtaining the thermal mass of the quarks as [12–14]:

$$\begin{aligned} H(k, T) &= [k^2 + m^2(T)]^{1/2} \\ &= k + m^2(T)/2k \quad \text{for large } k \end{aligned} \quad (1)$$

where ,

$$\begin{aligned} m^2(T) &= 16\pi\gamma_{qq} \alpha_s(k)T^2 \left[1 + \frac{\alpha_s(k)}{4\pi} a_1 \right. \\ &\quad \left. + \frac{\alpha_s^2(k)}{16\pi^2} a_2 + \frac{\alpha_s^3(k)}{64\pi^3} a_3 \right]. \end{aligned} \quad (2)$$

where $\gamma_{qq} = \frac{\sqrt{(\gamma_q^2 + \gamma_g^2)}}{\gamma_q \gamma_g}$ with $\gamma_q = 1/10$ and $\gamma_g = 60\gamma_q$. The mass is called thermal mass and it is obtained after the three loop corrections being introduced in the potential. The corresponding co-efficients obtained in thermal mass are a_1 , a_2 and a_3 . These are obtained by the interactions among the constituent particles through the loop corrections. These are numerically found to be depending on the number of quark flavours and they are given as:

$$a_1 = 2.5833 - 0.2778 n_l, \quad (3)$$

$$a_2 = 28.5468 - 4.1471 n_l + 0.0772 n_l^2, \quad (4)$$

$$a_3 = 209.884 - 51.4048 n_l + 2.9061 n_l^2 - 0.0214 n_l^3 \quad (5)$$

where n_l is considered to be the number of light quark elements [15–18]. k is the quark (gluon) momentum. The loop co-efficients a_1, a_2 and a_3 play the roles for involving in the creation of QGP energy and formation of QGP

droplet. Due to these co-efficients, we found the different quark and gluon parametrization factors in forming the QGP droplets. The parametrization factors are obtained as $\gamma_q = 1/14$ and $\gamma_g = (60 - 70) \gamma_q$ in obtaining the stable droplets. It indicates that the overall calculation is controlled with the most favourable results in all properties. The value varies from small to large depending on non-loop to loop correction. $\alpha_s(k)$ is QCD running coupling constant defined as:

$$\alpha_s(k) = \frac{4\pi}{(33 - 2n_f) \ln(1 + k^2/\Lambda^2)}, \quad (6)$$

in which Λ is QCD parameter almost equal to 0.15 GeV. n_f is degree of freedom of quark and gluon. So the interacting mean-field potential $V_{conf}(k)$ is derived with inclusion of one to three loop corrections. In the derivation of the potential, the expansion of strong coupling constant through the one to three loop factors is used with the technique of the perturbation theory [19–23].

$$\begin{aligned} V_{conf}(k) &= \frac{8\pi}{k} \gamma_{qq} \alpha_s(k) T^2 \left[1 + \frac{\alpha_s(k) a_1}{4\pi} + \frac{\alpha_s^2(k) a_2}{16\pi^2} \right. \\ &\quad \left. + \frac{\alpha_s^3(k)}{64\pi^3} a_3 \right] - \frac{m_0^2}{2k}, \end{aligned} \quad (7)$$

Now the density of states in phase space with loop corrections in the interacting potential is obtained as [14, 24–27]:

$$\rho_{q,g}(k) = \frac{v^2}{3\pi^2} \frac{dV_{conf}^3(k)}{dk}, \quad (8)$$

or,

$$\rho_{q,g}(k) = \frac{v^2 g^6(k)}{8\pi^2 k^4} \gamma_{qq}^3 T^6 \left[1 + \frac{\alpha_s(k) a_1}{\pi} + \frac{\alpha_s^2(k) a_2}{\pi^2} + \frac{\alpha_s^3(k) a_3}{\pi^3}\right]^2 B, \quad (9)$$

where

$$\begin{aligned} B &= \left\{ \left[1 + \frac{\alpha_s(k) a_1}{\pi} + \frac{\alpha_s^2(k) a_2}{\pi^2} + \frac{\alpha_s^3(k) a_3}{\pi^3}\right] \right. \\ &\quad \left. + \frac{2k^2}{\Lambda^2 + k^2} \left\{ \frac{(1 + 2\alpha_s(k) a_1/\pi)}{\ln(1 + k^2/\Lambda^2)} + \frac{3\alpha_s^2(k) a_2}{\pi^2} \right. \right. \\ &\quad \left. \left. + \frac{4\alpha_s^3(k)}{\pi^3} \frac{a_3}{\ln(1 + k^2/\Lambda^2)} \right\} \right\} \end{aligned} \quad (10)$$

and v is the volume occupied by the QGP and $g^2(k) = 4\pi\alpha_s(k)$.

III. THE FREE ENERGY AND SURFACE TENSION WITH LOOP CORRECTIONS

The fermion and boson free energy after incorporating one to three loop corrections in the density of state is [28]:

$$F_i = -\eta T g_i \int dk \rho_{q,g}(k) \ln(1 + \eta e^{-\sqrt{m_i^2 + k^2}/T}), \quad (11)$$

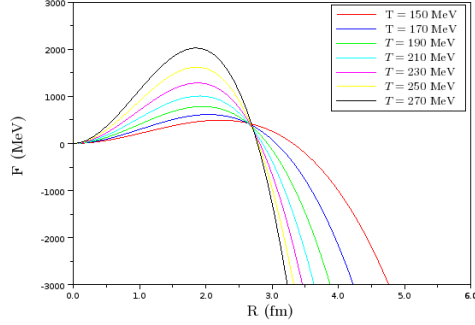


FIG. 1: The free energy vs. R at $\gamma_q = 1/14$, $\gamma_g = 60\gamma_q$ for various values of temperature.

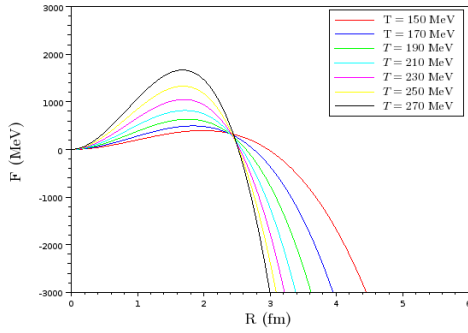


FIG. 2: The free energy vs. R at $\gamma_q = 1/14$, $\gamma_g = 64\gamma_q$ for the various values of temperature.

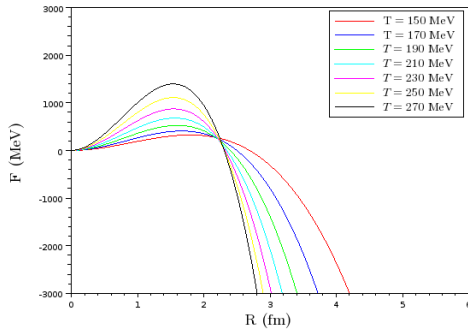


FIG. 3: The free energy vs. R at $\gamma_q = 1/14$, $\gamma_g = 68\gamma_q$ for the various values of temperature.

where $\eta = +ve$ gives the contribution of bosonic particle and $\eta = -ve$ gives the contribution of the fermionic particles. The extreme in the potential with minimal approximation is obtained by minimizing the confining potential in terms of momentum and it is approximately defined as:

$$V(k_{min}) = \left[\frac{8a_1\gamma_{qg}N^{\frac{1}{3}}T^2\Lambda^4}{27\pi^2} \right]^{1/6}, \quad (12)$$

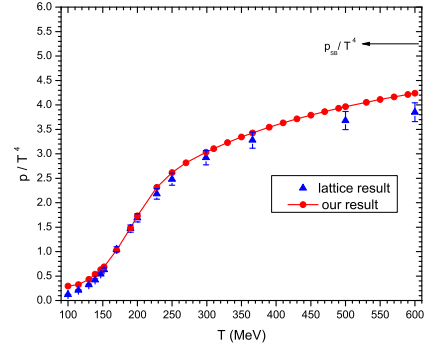


FIG. 4: Pressure vs. T at $\gamma_q = 1/14$, $\gamma_g = 68\gamma_q$.

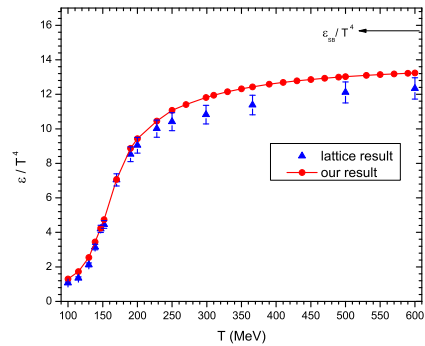


FIG. 5: Energy density vs. T at $\gamma_q = 1/14$, $\gamma_g = 68\gamma_q$.

where $N = (4/3)[12\pi/(33 - 2n_f)]$. Yet in this brief paper the cut off potential is taken differently from the above value of minimum potential in order to get more closer result to lattice. Due to the appropriate choice of this minimum value we get more similar outputs to lattice with the larger contribution in the entire calculation of free energy of boson and fermion. It implies that the minimum cut off in the integral tends to produce highly

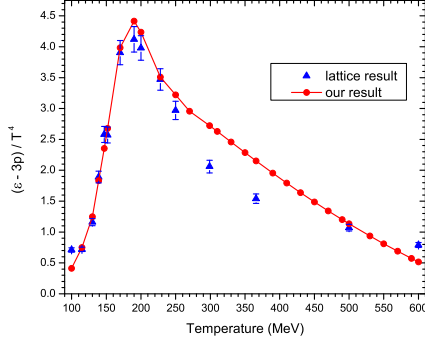


FIG. 6: Interaction measurement vs. T at $\gamma_q = 1/14$, $\gamma_g = 68\gamma_q$.

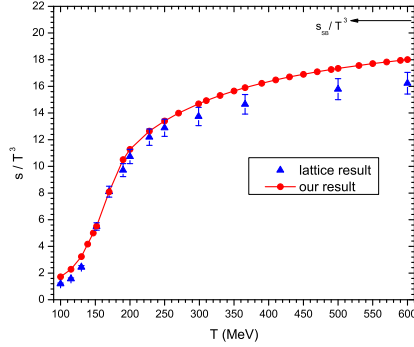


FIG. 7: Entropy vs. T at $\gamma_q = 1/14$, $\gamma_g = 68\gamma_q$.

accurate in energy spectrum of fermion and boson. It also helps in erasing the infra-red divergence of the integration in evaluation with the magnitude of Λ and T . g_i is degeneracy factor (color and particle-antiparticle degeneracy) which is 6 for quarks and 8 for gluons. The inter-facial energy obtained through Ramanathan et al's

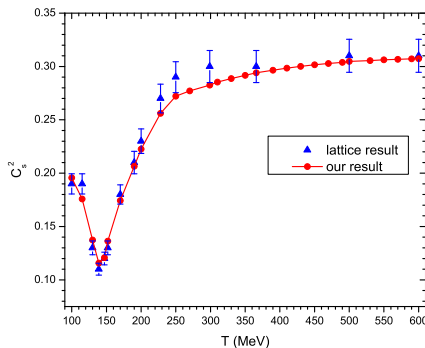


FIG. 8: Speed of sound vs. T at $\gamma_q = 1/14$, $\gamma_g = 68\gamma_q$.

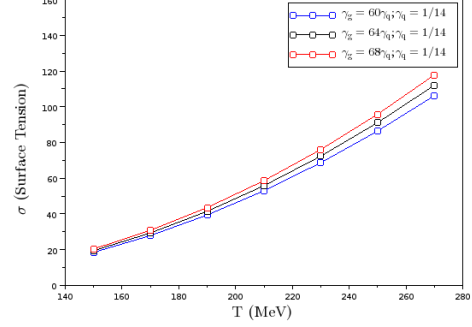


FIG. 9: The Surface Tension vs. T at $\gamma_q = 1/14$, different γ_g .

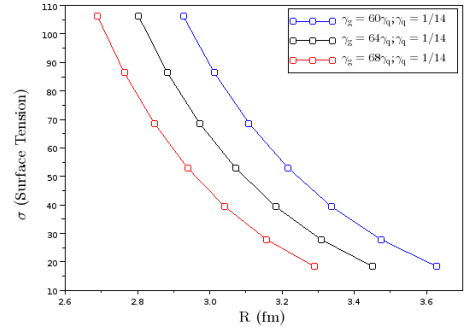


FIG. 10: The Surface Tension vs. R at $\gamma_q = 1/14$, different γ_g .

model [19, 29] with a suitable parameter of the hydrodynamic effects is also given as:

$$F_{interface} = \frac{1}{4}\gamma_{qg}R^2T^3. \quad (13)$$

The energy is used to replace the bag energy of MIT model. It gives minimum shortfall in comparison to the energy used by MIT model. In addition to these particles,

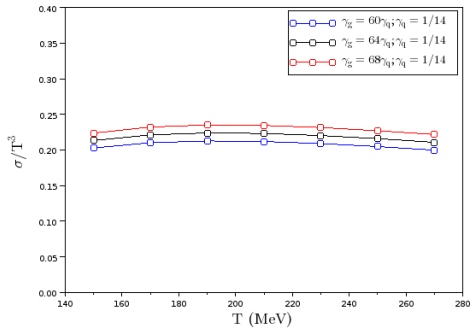


FIG. 11: The Surface Tension/ T_c^3 vs. T at $\gamma_q = 1/14$, different γ_g .

we add some light particle hadrons and the corresponding energies are calculated using their masses [30]

$$F_h = (d_i T / 2\pi^2) v \int_0^\infty k^2 dk \ln(1 - e^{-\sqrt{m_h^2 + k^2}/T}). \quad (14)$$

where d_i is the degeneracy factor for the different light hadronic particles and m_h is the light hadron corresponding masses. Here we use only maximum light hadron as their involvement in the reaction plane is more dominant during the time of collision. So total fermions involved in system are taken as: dynamical quark masses $m_u = m_d = 0 \text{ MeV}$ and $m_s = 0.15 \text{ GeV}$. Therefore the total free energy F_{total} as a combination of fermion and boson is as:

$$F_{total} = \sum_j F_j + F_h, \quad (15)$$

where j stands for u, d, s quark, interface and gluon.

We further calculate the surface tension of QGP fireball under the three loop correction and as before, the evaluation is done by the difference of free energy between QGP phase and the light element hadrons phase. It implies that there is a sharp boundary between hadron and quark phase, neglecting the short life mixed phase which really balance the pressure and keep the system in chemical equilibrium. Though it has been reported the importance of the mixed phase in the calculation of surface tension due to large finite size and its effects disturbed on the surface tension [31, 32]. So the difference in energy of the two phases is defined after neglecting the finite size effects and shape contribution. It is therefore given as:

$$\Delta F = -\frac{4\pi}{3} R^3 \Delta P + 4\pi R^2 \sigma \quad (16)$$

where the first term represents pressure difference between QGP matter and hadronic matter. The second term represents the contribution from the surface tension. The surface tension is evaluated through the minimizing process of the above expression with respect to droplet size R . So, the surface tension formula is obtained as:

$$R_c = \frac{2\sigma}{\Delta P} \text{ or } \sigma = \frac{3\Delta F}{4\pi R_c^2} \quad (17)$$

where, ΔF is the change in the free energy and R_c is the corresponding critical radius obtained at the transition point from quark droplet to hadron droplet.

IV. RESULTS:

The free energy calculation is done through the inclusion of three loop to our earlier one loop correction model in the interacting mean-field potential. The calculated outputs are represented by the corresponding figures. Due to the inclusion of loop corrections, the free

energy evolution of QGP droplet changes a lot in terms of its amplitude as well as the stability of droplet formation. The droplet sizes are found to be slightly changed with the droplet size. This size is accordingly obtained with the parametrization factor introduced in the model. The free energies are therefore shown in the figures 1,2 and 3 with the different parameter factors and their stability also increases with the change of gluon flow parameters. It indicates that the parameters really play a significant role to regularize the stability of the droplets and it acts as a magic number in modeling the fluid dynamics. In Fig.1, we show the free energy of QGP droplet at the particular quark and gluon flow parametrization factor $\gamma_q = 1/14$, $\gamma_g = 60\gamma_q$. Similarly, in Fig.2 it is free energy of QGP droplet with slightly lesser stability from the figure1. The droplet is obtained at the quark and gluon flow parameter $\gamma_q = 1/14$, $\gamma_g = 64\gamma_q$. Again we plot free energy with increased gluon flow parameter. In Fig.3 the stability of droplet is lesser, yet the droplet is obtained at the parametrization factor $\gamma_q = 1/14$, $\gamma_g = 68\gamma_q$. So we get a number of free energy evolution at different parameters showing a slight difference in the stability of droplet. Choosing one of the best stable droplet, then we try to picture the thermodynamic characteristics of the particular droplet at the particular parameter value. These thermodynamics are presented by the equation of state (EOS), pressure, interaction measurement, entropy, speed of sound and the surface tension with radius and temperature. These are shown in the figures.

In Fig.4 we see the pressure with the variation of temperature and the plot is compared with the lattice data. The pressure is almost similar with the lattice. In order to obtain a better result much closer to the lattice data the minimum cut off of the integration has been modified with the rescale momentum rather than taking the exact minimum momentum cut off. If we put the the exact minimum cut off then pressure at higher temperature does not change and match with the lattice but at low temperature it becomes very large. Therefore, in order to keep the results closer to lattice from low to high temperature a necessary modification has been introduced according to momentum and temperature.

Similarly in Fig.5 we plot the energy density of our model and compare with the lattice. Here the result is again similar in the entire range of temperature. This is also done with same scale in the integration of energy density. It indicated that the model has a little drawback at the lower temperature as the energy density is higher in comparison with lattice if we look into our earlier cut off value. By changing the cut off to scale of the lattice the model completely fit the the spectrum of the lattice trajectory.

Now by looking these above two plots in Fig.6, we plot the interaction measurement with the temperature again. In the plot there is no much difference with the result produced by the lattice data. This indicates that the model can describe the QCD phase structure in a very good way by modifying the cut off in the integration of the

free energy and other thermodynamic relations. In the model we need very small value of lower limit calculating from theoretical expression and it then gives the different pictures in the spectrum of QCD phase structure. In the lower value, it gives higher value and as the limit is higher then it approximately falls to the lattice. It is the reason that at higher temperature the result produced by the present model lies within the range of the comparative results [33].

Now we see the entropy picture and it is shown in Fig.7. Entropy follows the same output of the lattice. This represents a good presentation about the order of equilibrium. So the system has stable flow in its movement from deconfined phase of QGP to confining phase of hadrons. Again we plot the speed of sound and it is shown in Fig.8. Our data is compared with the lattice data. The speed of sound absolutely follows the same curve traced by the lattice. It indicates that the speed of sound in our model results in producing almost the exact solution in the transformation of the QGP fluid movement producing the ideal liquid flow.

Now we look at the stability formation of the droplets. We plot the different figures 9, 10 and 11 of the surface tension. These are the characteristic features to explain the surface tension. Fig.9 shows the variation of the surface tension with the size of droplet. As the size of droplet increases the surface tension decreases and somewhere the droplet disappear and no surface tension is obtained. This can be shown that the surface tension tends to reach the horizontal axis representing the size of the droplet. Again in Fig.10 we plot the surface tension with the variation of temperature. As the temperature of the system increases the surface tension is found to be linearly increasing due to the formation of smaller size of the droplet. At the larger temperature, it can be identified from the free energy formation that the size of the droplet is decreased with the increasing temperature. For the smaller temperature the size is large leading to smaller value of the surface tension. This is the property of liquid drop formation. At last in Fig.11 we plot the the constancy of the surface tension as indicated by the other model that there is constancy if we look the plot of σ/T^3 with temperature T . The result is shown in our earlier paper also. This indicates that the model is quite competent to explain the QCD phase structure and other thermodynamic pictures after a simple modification in the lower cut off of the integration of free energy with the scale of the lattice to obtain more closer results with the lattice data [34–36] So the inclusion of three loop correction in the mean field potential improve with increasing parameters and enhance the stability of QGP droplet with a slight modification in the cut off of the integration with the scale of the larger momentum.

The parameter obtained with the three loop represents

Reynold's like number showing the characteristic features of fluid dynamics and these type of parameter can be reproduced depending on the fluid. So in QGP fluid of early universe expansion, we have such parameters to explain the equilibrium movement of the QGP dynamics. It means quark and gluon parameter may have some other characteristic features to determine the stability formation of QGP droplets.

V. CONCLUSION:

The results show the formation of free energy and its improvement by the presence of three loop correction in the mean field potential. The effects on droplet formation is increased with the increase in stability when the loop correction is increased. These results are indicated by the figures of 1 to 3 with the increase in the parametrization values. As the loop correction is increased the free energy formation is also increased depending on the number of particles involved in the system. This has been observed from our earlier works that in one and two loop correction we have obtained different size of the droplets depending on the constituent particles. So the formation of stable droplet is effected by the parameter factor and particles. Taking into account of all these factor, we attempt to produce more closer results to lattice and we produce very much similar results by approximating the number of particles and the lower cut off value of the momentum. In addition to these results, we represents the thermodynamic properties and surface tension to picture the QCD phase structure and the stability of the droplets. The correction of three loop really enhances more in all the thermodynamics relations in comparison to two loop and one correction and it is more closer toward the lattice results [7,17]. It indicates that our simple model with three loop correction with the dynamical flow parameter can produce better EOS of QCD and enhance the stable droplet formation and thus the possible solution is that the evolution of QGP fireball is more steady fluid dynamics depending on some kind of dynamical parameter representing the characteristic features of forming the stable droplets.

A. Acknowledgments:

We thank the retired Prof. R. Ramanathan for giving valuable time in discussion about the manuscript's complete form. The author, S. S. Singh thanks the university for providing research and development grants for this work successful.

- Phys. Lett. B 264, 213 (1991).
- [3] F. H. Lin, S. Fakhraddin, E. S. Grinbaun, B. K. Singh, Art. ID 190908 (2015).
- [4] S. Dash, B. K. Nandi, R. Nayal, A. K. Pandey, P. Sett, Mod. Phys. Lett. A, 32, 1750060 (2017).
- [5] Satz H 1978 *CERN-TH-2590* 18pp.
- [6] Karsch F, Laermann E, Peikert A, Schmidt Chand Sticksan S 2001 *Nucl. Phys. B* **94**, 411.
- [7] Karsch F and Satz H, 2002 *Nucl. Phys. A* **702**, 373.
- [8] S. S. Singh, Ramanathan R, 2014 *Prog. Th. Expt. Phys.* *103D02*.
- [9] S. S. Singh, G, Saxena, Pramana J. Phys 92, 68 (2019).
- [10] S. S. Singh and Saxena G, 2017 *Pramana J Phys.* **85**
- [11] S. S. Singh and Ramanathan, 2018 *Ind J Phys.* **92(2)** 245.
- [12] Peshier A, Kämpfer B, Pavlenko O P and Soff G, 1994 *Phys. Lett. B* **337**, 235.
- [13] Goloviznin V and Satz H, 1993 *Z. Phys. C* **57**, 671.
- [14] Ramanathan R, Mathur Y K, Gupta K K and Jha A K, 2004 *Phys. Rev. C* **70**, 027903.
- [15] Fischler W, 1977 *Nucl. Phys. B* **129**, 157.
- [16] Billoire A, 1980 *Phys. Lett B* **92**, 343.
- [17] Smirnov A V, Smirnov V A, Steinhäuser M, 2008 *Phys. Lett. B* **668**, 293.
- [18] Smirnov A V, Smirnov V A and Steinhäuser M, 2010 *Phys. Rev. Lett.* **104**, 112002.
- [19] Ramanathan R, Gupta K K, Jha A K and Singh S S, 2007 *Pramana J. Phys.* **68**, 757.
- [20] Brambilla N, Pineda A, Soto J and Vairo A, 2001 *Phys. Rev D* **63**, 014023.
- [21] Melnikov K and Yelkhovsky A, 1998 *Nucl. Phys. B* **528**, 59.
- [22] Hoang A H, 1999 *Phys. Rev D* **59**, 014039.
- [23] V. A. Yerokhin, P. Indelicato, V. M. Shabaev, 2007 *Can. J. Phy* **85**, 251.
- [24] Linde A D, 1983 *Nucl. Phys. B* **216**, 421.
- [25] Fermi E, 1928 *Zeit F. Physik* **48**, 73.
- [26] Thomas L H, 1927 *Proc. Camb. Phil. Soc.* **23**, 542.
- [27] Bethe H A, 1937 *Rev. Mod. Phys.* **9**, 69.
- [28] Christiansen M B and Madsen J, 1997 *J. Phys. G: Nucl. Par. Phys* **23**, 2039.
- [29] Weyl H, 1911 *Nachr. Akad. Wiss Gottingen* 110.
- [30] Balian R and Block C, 1970 *Ann. Phys. (NY)* **60**, 401.
- [31] Yasutake N, Maruyama T, Tatsumi T, 2011 *J. Phys. Conf. Series* **312** 042027.
- [32] S S.Singh, Gupta K K, Jha A K, 2014 *Int. J. Mod. Phys. A* **29** 1450097.
- [33] D. S. Gosain and S. S. Singh, 2014 *Intrn. J. Theo. Phys* **53** 2688.
- [34] Kajantie K, Kärkkäinen L and Rummukainen K, 1990 *Nucl. Phys. B* **333** 100.
- [35] Iwasaki Y, Kanaya K, Kärkkäinen L, Rummukainen K and Yoshié T, 1994 *Phys. Rev. D* **49** 3540.
- [36] Christiansen M B and Madsen J, 1996 *Phys. Rev. D* **53** 5446.